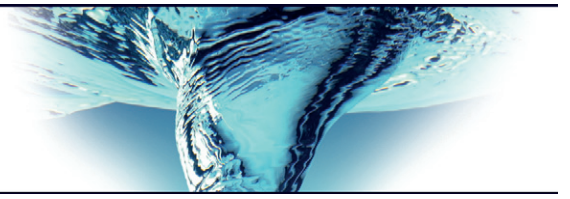
CrossMark

J. Fluid Mech. (2018), *vol.* 840, R1, doi:10.1017/jfm.2018.92



JFM RAPIDS
journals.cambridge.org/rapids

Onset conditions for vortex breakdown in supersonic flows

Toshihiko Hiejima†

Department of Aerospace Engineering, Osaka Prefecture University, 1-1 Gakuen-cho, Nakaku, Sakai, Osaka 599-8531, Japan

(Received 18 September 2017; revised 27 November 2017; accepted 16 January 2018; first published online 6 February 2018)

This study proposes an onset condition of shock-free supersonic vortex breakdown from the axial momentum variation, which applies in the presence or absence of a stagnation point. The condition is derived from a comprehensive approach to vortex breakdown. Supersonic breakdown appeared when the swirl parameter and Mach number were small. Moreover, bubble-type breakdowns with a stagnation point, which occur in subsonic conditions, could not occur under the supersonic condition in the present analysis. The predicted breakdowns under this condition were consistent with the results of the three-dimensional numerical simulations for Mach numbers ranging from 1.5 to 5.0. Supersonic vortex breakdowns were clearly captured by the helicity contours in the numerical results. The threshold of the downstream Mach number required for spiral breakdown with no stagnation point was also theoretically derived and verified in numerical results. These findings provide new insights into vortex breakdown in supersonic flows.

Key words: compressible flows, vortex breakdown, vortex flows

1. Introduction

Since future-generation aeroplanes must exploit the characteristics of supersonic flow in high-speed airstreams, it is essential to deploy delta wings. Several decades ago, vortex breakdown over delta wings and in pipe flows was discovered as a sudden bursting of swirling flows. Wing-tip vortex breakdown over delta wings is detailed in Nelson & Pelletier (2003). Vortex breakdown manifests as a sudden increase in core size, a large adverse pressure gradient, a stagnation point formed near the axis, flow reversal and a highly unstable structure (Hall 1972; Leibovich 1978; Escudier 1988; Delery 1994; Lucca-Negro & O'Doherty 2001). Vortex breakdown has also been viewed as a fold catastrophe (Shtern & Hussain 1999). In many incompressible flow studies, the onset of vortex breakdown was found to be governed by the swirl

† Email address for correspondence: hiejima@aero.osakafu-u.ac.jp

© Cambridge University Press 2018

https://doi.org/10.1017/jfm.2018.92 Published online by Cambridge University Press

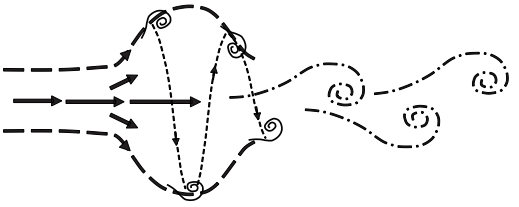


FIGURE 1. Schematic of streamwise vortex breakdown with axial velocity acceleration in supersonic cases. Reprinted with permission from Hiejima, *Phys. Fluids* **29**, 054102 (2017). Copyright 2017 American Institute of Physics.

strength, i.e. the swirl number or the Rossby number. In contrast, a few studies on compressible vortex breakdowns have yielded contradictory results. In some studies, the critical swirl number in subsonic flows was found to increase with Mach number (Visbal & Gordnier 1995; Rusak & Lee 2002; Herrada, Pérez-Saborid & Barrero 2003). Other studies have reported the opposite result, such as shock-induced breakdown (Keller 1994; Mahesh 1996; Luginsland & Kleiser 2015). Furthermore, in shock-free supersonic flows, where the Mach number is greater than unity, the outbreak mechanism of vortex breakdown remains to be identified.

The critical conditions for vortex breakdown have been studied in various theoretical frameworks. Assuming that vortex breakdown occurs by a similar process to hydraulic jumps and shockwaves, Benjamin (1962) proposed that vortex breakdown represents a transition from supercritical to subcritical flows under bounded flows. A supercritical flow supports only downstream travelling waves, whereas a subcritical flow supports both upstream and downstream travelling waves. Mager (1972) and Ruith *et al.* (2003) applied Benjamin's analysis to radially unbounded flows. Escudier (1988) proposed a two-stage transition when the angular momentum is conserved along the stream surfaces. Keller (1994) extended this method to the compressible case. By observing the size of the vortex core, Darmofal *et al.* (2001) estimated the breakdown conditions by a quasi-one-dimensional approach using the flux-averaged stagnation pressure in confined and unconfined geometries. Assuming axial momentum conservation along the vortex axis, Mahesh (1996) derived critical swirl numbers from the pressure rise in supersonic flows. From the connection between spiral-type instabilities and vortex breakdown, it was also shown that the axial deceleration developed into a stagnation point (Ruith *et al.* 2003; Broadhurst & Sherwin 2008). Thus, it is believed that axial deceleration into a stagnation point precedes vortex breakdown in both subsonic and supersonic flows. However, when the stagnation point was assumed in theoretical investigations of breakdown onset, the verifications in compressible cases (including supersonic flows) were unsatisfactory. Indeed, the axial velocity is thought to accelerate during vortex breakdown in supersonic flows, as shown in figure 1 (Hiejima 2017). To seek the onset condition of comprehensive vortex breakdown without a stagnation point, it becomes necessary to consider the occurrence of vortex breakdown as the momentum variation response to the pressure rise as well as the increased velocity. This clarification is the theme of the present paper.

The purpose of this study is to estimate the onset conditions of vortex breakdown in supersonic flows. To this end, the present study proposes a new condition for shock-free supersonic vortex breakdown based on the axial momentum rise along the vortex axis, without assuming a stagnation point. The theoretical condition is verified in three-dimensional numerical simulations.

https://doi.org/10.1017/jfm.2018.92 Published online by Cambridge University Press

2. Basic flows

To investigate breakdown of supersonic streamwise vortices, Batchelor vortices (Batchelor 1964) are applied because their profiles are compatible with many swirling flows. The radial, azimuthal and axial velocities (u_r, u_θ and u_x) of the Batchelor vortex are, respectively, given by

$$u_r(r) = 0, \quad u_\theta(r) = \frac{q}{r}[1 - \exp(-r^2)], \quad u_x(r) = 1 - \mu \exp(-r^2), \quad (2.1a\text{–}c)$$

where q and μ denote the swirl intensity (circulation) and axial velocity deficit, respectively, and their ratio defines the swirl parameter $\Phi = q/\mu$, which presents a similarity feature in instability (Hiejima 2013). The density $\rho(r)$ and pressure $p(r)$ required for supersonic conditions in a basic inviscid steady flow are, respectively, given by

$$\frac{\mathrm{d}p}{\mathrm{d}r} = \rho \frac{{u_\theta}^2}{r}, \quad \frac{\mathrm{d}\rho}{\mathrm{d}r} = \frac{\rho}{\gamma}\left(\frac{1}{p}\frac{\mathrm{d}p}{\mathrm{d}r} - \frac{\mathrm{d}s}{\mathrm{d}r}\right), \quad (2.2a,b)$$

where s is the entropy and γ is the ratio of the specific heats. The entropy gradient in (2.2) is described by the Crocco equation on the assumption that the stagnation temperature is uniform (Hiejima 2013).

3. Onset conditions for vortex breakdown

Although the swirl intensity at the upstream is an important condition for vortex breakdown, the swirl number is upper-bounded because the static pressure is positive in a compressible flow. A strong swirl causes low pressure along the axis and results in momentum reduction there. An axial velocity deficit can also create a similar effect to momentum reduction. The occurrence of vortex breakdown seems to be related to low momentum on the upstream vortex axis. From a momentum perspective, a pressure rise and an increased axial velocity at the downstream are regarded as an increase in momentum. This is a key for the onset condition of universal vortex breakdown. The momentum increase caused by vortex breakdown can be interpreted as follows. In cylindrical polar coordinates, the conservation of mass equation is

$$\frac{\partial(\rho)}{\partial t} + \frac{1}{r}\frac{\partial(r\rho u_r)}{\partial r} + \frac{1}{r}\frac{\partial(r\rho u_\theta)}{\partial \theta} + \frac{\partial(\rho u_x)\rho u_x}{\partial x} = 0. \quad (3.1)$$

According to Darmofal (Mahesh 1996), vortex breakdown is regarded as an inviscid transition at Reynolds number above 300. In terms of the axial momentum J, the conservation of momentum equation becomes

$$\frac{\partial(\rho u_x)}{\partial t} + \frac{1}{r}\frac{\partial(r\rho u_r u_x)}{\partial r} + \frac{1}{r}\frac{\partial(r\rho u_\theta u_x)}{\partial \theta} + \frac{\partial J}{\partial x} = 0. \quad (3.2)$$

Inviscid vortex breakdown is a transition between two conjugate flow states (Benjamin 1962; Mager 1972). Brown & Lopez (1990) derived the physical mechanism of incompressible vortex breakdown from the momentum equation. In steady flows where $u_\theta(0) \approx 0$ along the axis, the axial momentum gradient can be approximated

https://doi.org/10.1017/jfm.2018.92 Published online by Cambridge University Press

by integrating (3.2) with respect to x and disregarding the unimportant terms using (3.1). The resulting approximation is

$$J_2 - J_1 \simeq \int_1^2 u_x \frac{\partial(-\rho u_r)}{\partial r}\,\mathrm{d}x. \tag{3.3}$$

Here, the indices 1 and 2 denote the upstream and downstream points, respectively. This expression describes a momentum increase caused by the radial spread of u_r.

Because a transition induces a large momentum increase in the streamwise direction, the momentum variation along the axis is crucially important. If the momentum difference between the upstream and downstream exceeds a certain fraction of the difference between the maximum and upstream momenta, then vortex breakdown is assumed to occur. The onset condition of vortex breakdown is given by

$$J_2 - J_1 - \alpha\,(J_{max} - J_1) > 0, \tag{3.4}$$

where the axial momentum is defined as $J_i = \rho_i u_i^2 + p_i = p_i(\gamma M_i^2 + 1)$ and the Mach number is $M_i = u_i/\sqrt{\gamma p_i/\rho_i}$. The maximum momentum can be reasonably assumed as $J_{max} \simeq J_\infty$. The subscript ∞ denotes a point at infinite radius (i.e. the free-stream state). As a comprehensive approach to the condition, the coefficient α is determined from the critical swirl number of incompressible vortex breakdown.

In incompressible vortex breakdown with a stagnation point, assuming $u_2 = 0$ and constant density, equation (3.4) becomes

$$p_2 - (p_1 + \rho u_1^2) - \alpha\,(p_\infty + \rho u_\infty^2 - p_1 - \rho u_1^2) > 0. \tag{3.5}$$

As is commonly assumed, the stagnation pressure at incompressible vortex breakdown was taken as $p_2 = p_\infty + 1/2\rho u_\infty^2$.

$$(1-\alpha)(p_\infty - p_1) > (1-\alpha)\rho u_1^2 + (\alpha - \tfrac{1}{2})\rho u_\infty^2. \tag{3.6}$$

Integrating the radial momentum equation (2.2) at the upstream, we obtain

$$p_\infty - p_1 = \rho \int_0^\infty \frac{u_\theta^2}{r}\,\mathrm{d}r = \rho\, q^2 \int_0^\infty \frac{1 - \exp(-r^2)}{r^3}\,\mathrm{d}r = \rho\, q^2 I(\infty). \tag{3.7}$$

Substituting (3.7) into (3.6), we then obtain

$$q^2 > \frac{u_\infty^2}{I(\infty)}\left[(1-\mu)^2 + \frac{2\alpha - 1}{2(1-\alpha)}\right]. \tag{3.8}$$

In accordance with previous theoretical works, we assume uniform axial velocity of the primary flow (i.e. $\mu = 0$). The critical swirl intensity is then given by

$$q > q_c = \frac{u_\infty}{\sqrt{2(1-\alpha)I(\infty)}}. \tag{3.9}$$

Here, q_c denotes the critical swirl intensity and r_c is the site of maximum azimuthal velocity. In many investigations into incompressible vortex breakdown, the critical swirl number $S_c = q_c/(r_c\, u_\infty)$ was determined as 1.4 (see, for instance, Delery 1994). From (3.9) and setting $r_c = 1.121$ for the Batchelor vortex in (2.1), we obtain $\alpha = 0.7066 \simeq 1/\sqrt{2}$ at vortex breakdown.

https://doi.org/10.1017/jfm.2018.92 Published online by Cambridge University Press

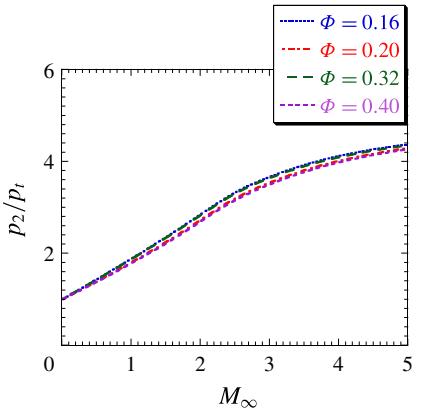


FIGURE 2. Downstream stagnation pressure necessary for vortex breakdown calculated by (3.10) as a function of M_∞ for $\Phi = 0.16, 0.20, 0.32$ and 0.40.

Note that the downstream momentum J_2 is unknown in (3.4). First, consider a vortex breakdown in which a stagnation point occurs under the above onset condition. The critical pressure p_2 is obtained by substituting $M_2 = 0$ into (3.4) as follows:

$$\frac{p_2}{p_t} = \alpha \frac{1 + \gamma M_\infty^2}{1 + \dfrac{\gamma - 1}{2} M_\infty^2} + (1 - \alpha) \frac{p_1}{p_\infty} \frac{1 + \gamma M_1^2}{1 + \dfrac{\gamma - 1}{2} M_\infty^2}, \tag{3.10}$$

where $p_t = p_\infty(1 + ((\gamma - 1)/2)M_\infty^2)$. The downstream stagnation pressures necessary for vortex breakdown, obtained from (3.10), are plotted as functions of M_∞ in figure 2. Here Φ ranges from 0.16 to 0.40. Although $p_2 = p_t$ in incompressible cases (at most $p_2 < 1.8\,p_t$ in subsonic cases), the downstream pressure p_2 required for breakdown increases several-fold as the Mach number increases. The required q deduced from the pressure difference at high stagnation pressure exceeds the maximum swirl number in compressible flows, which is limited as mentioned above. This suggests that vortex breakdown with a stagnation point cannot occur in supersonic flows.

Next, consider a vortex breakdown without stagnation points. In supersonic vortex breakdown, the axial velocity accelerates along the vortex axis. In vortex breakdown without stagnation points, suppose that $p_2 \simeq p_1$ because $\partial p/\partial x$ exerts a weak effect (Hiejima 2017, figure 7). Applying $p_2 = p_1$ to (3.4), the critical downstream Mach number M_2 is expressed as

$$F(M_2) = \frac{M_2^2 - \beta M_1^2}{M_\infty^2} - \frac{\alpha \hat{I}(\infty)}{p_1} \left(1 + \frac{1}{\gamma M_\infty^2}\right) q^2, \tag{3.11}$$

$$p_\infty - p_1 = q^2 \hat{I}(\infty) = \int_0^\infty \rho \frac{u_\theta^2}{r}\, \mathrm{d}r, \tag{3.12}$$

where $\beta = 1 - \alpha$. Equation (3.11) is constant independent of M_∞ for various Φ ($q = 0.08$–0.32, $\mu = 0.2$–1.0); $F(M_2) = \alpha$. Therefore, the critical M_2 for supersonic vortex breakdown can be simply expressed.

https://doi.org/10.1017/jfm.2018.92 Published online by Cambridge University Press

4. Supersonic vortex breakdown obtained from numerical simulations

To verify the onset condition in § 3, the breakdowns of streamwise vortices were numerically investigated at various Mach numbers 1.5–5.0. The governing equations were the three-dimensional, unsteady compressible Navier–Stokes equations in general coordinates and were discretised by a finite difference scheme. The normalisation of the physical variables and the numerical method are described in Hiejima (2017). The Reynolds number based on the sonic velocity is 4500 and the Prandtl number is 0.72. The physical domain was a rectangular box with sides $L_x = 300$ and $L_y = L_z = 40$. The spatial resolutions were $N_x = 901$ and $N_y = N_z = 171$, which proved sufficient for observing the transition process of streamwise vortices in previous work (Hiejima 2017). The inflows were fixed Batchelor vortices (described in § 2) with the addition of random noise. The maximum noise amplitude was set to be 3 % that of the magnitude of the free-stream variables. The parameters in (2.1) were set as follows: $\Phi = 0.16$ ($q = 0.08$, $\mu = 0.5$), $\Phi = 0.20$ ($q = 0.16$, $\mu = 0.8$), $\Phi = 0.32$ ($q = 0.16$, $\mu = 0.5$), and $\Phi = 0.40$ ($q = 0.32$, $\mu = 0.8$). Symmetry conditions were imposed at the boundary surfaces in the Y–Z cross-section. The outflow condition (where the flows were supersonic) was extrapolated to zeroth order.

To begin with, to visualise the presence or absence of supersonic vortex breakdown, the helicity density contours were computed in the X–Z cross-sections through the vortex axis for various Φ. The results for $M_\infty = 2.5$ and 3.5 are presented in figures 3 and 4, respectively. Note that the black part expresses the main vortical structure in swirling flows and the areas inside the red lines represent the subsonic domain. Spiral structures induced by the transitions develop around each main vortex, as observed in incompressible cases (Abid 2008; Broadhurst & Sherwin 2008). Note that, in figures 3(*a*,*b*) and 4(*a*), there are regions with no vortex axis, indicating that the vortices have broken down. Remarkably, in figure 4(*a*), breakdown occurs in the absence of subsonic regions with a pure supersonic state, and the disturbances are not propagated upstream. As the parameters Φ and M_∞ increase, the vortex axes are sustained downstream, and the vortical structures are not disrupted.

Next, the momentum variation along the axis was checked. Figure 5(*a*) shows the streamwise variations in axial momentum J/M_∞^2 at $M_\infty = 2.5$. The momentum increases are slight during normal transition (based on instabilities) but very large during vortex breakdown (strong transition). At $\Phi = 0.16$ and 0.20, vortex breakdown is evidenced by two features in the momentum distributions: a steep rise and a steady zone. The steep rise of the axial momentum is similar to the feature of incompressible breakdowns caused by the large pressure rise (Benjamin 1962; Ruith *et al.* 2003). The steady distribution was observed in earlier studies of vortex breakdown (Hiejima 2016, 2017). Thus, the momentum increases along the axis can be reasonably attributed to the occurrence of vortex breakdown. Figure 5(*b*) shows the streamwise energy variations along the axis at $M_\infty = 2.5$, calculated as follows:

$$E = \frac{1}{2} u_k u_k + \frac{\gamma}{\gamma - 1} \frac{p}{\rho}. \tag{4.1}$$

According to this figure, the energies are conserved from upstream to downstream even when breakdowns occur ($\Phi = 0.16$ and 0.20). This result is also important for theoretical formulations because the downstream state is usually unknown.

Figure 6 shows the axial vorticity and primitive variables in various planes perpendicular to the mainstream flow at $M_\infty = 2.5$ and $\Phi = 0.20$ (note that the vortex breaks down around $X = 100$). The non-zero u_y corresponding to the radial velocity

https://doi.org/10.1017/jfm.2018.92 Published online by Cambridge University Press

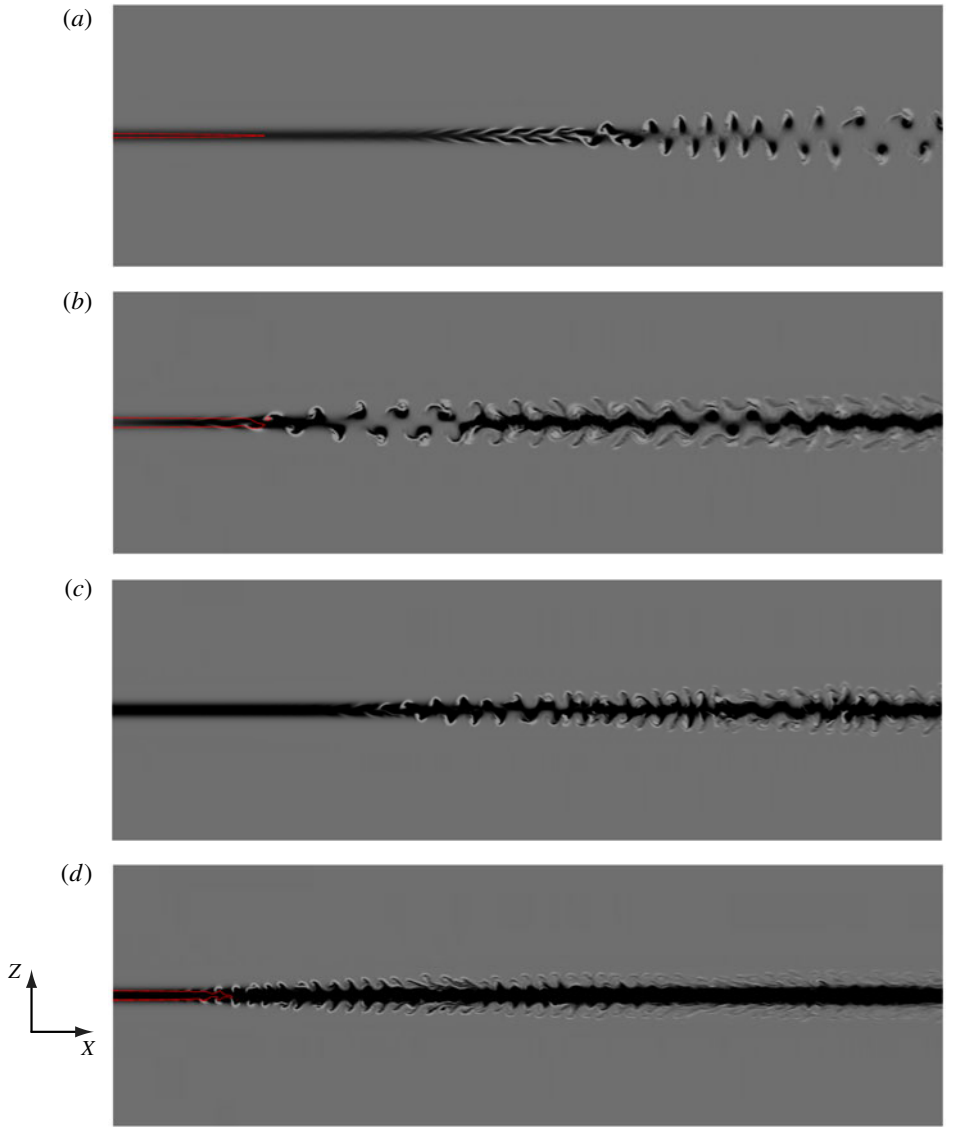


FIGURE 3. Transition processes of the streamwise vortices, described by the helicity density contours in the cross-sections through the vortex axis: (*a*) $\Phi = 0.16$, (*b*) 0.20, (*c*) 0.32 and (*d*) 0.40 at $M_\infty = 2.5$. Positive and negative helicities are rendered in black and white, respectively. Black regions indicate the main vortical structure in the swirling flows; the red lines enclose the subsonic domain.

indicates that vortex breakdown induces flow expansion. The axial velocity becomes steady at $X = 100$, where the axial vorticity vanishes, weakening u_z corresponding to the azimuthal velocity. The pressure and density profiles are also steady there. Mager (1972) stated that vortex breakdown distorts both the axial and the azimuthal velocity profiles, and almost equalises the static pressure in the core. Supersonic vortex breakdown is characterised not by a large pressure rise but by increased axial density; this finding has not been previously reported. Furthermore we find that when

https://doi.org/10.1017/jfm.2018.92 Published online by Cambridge University Press

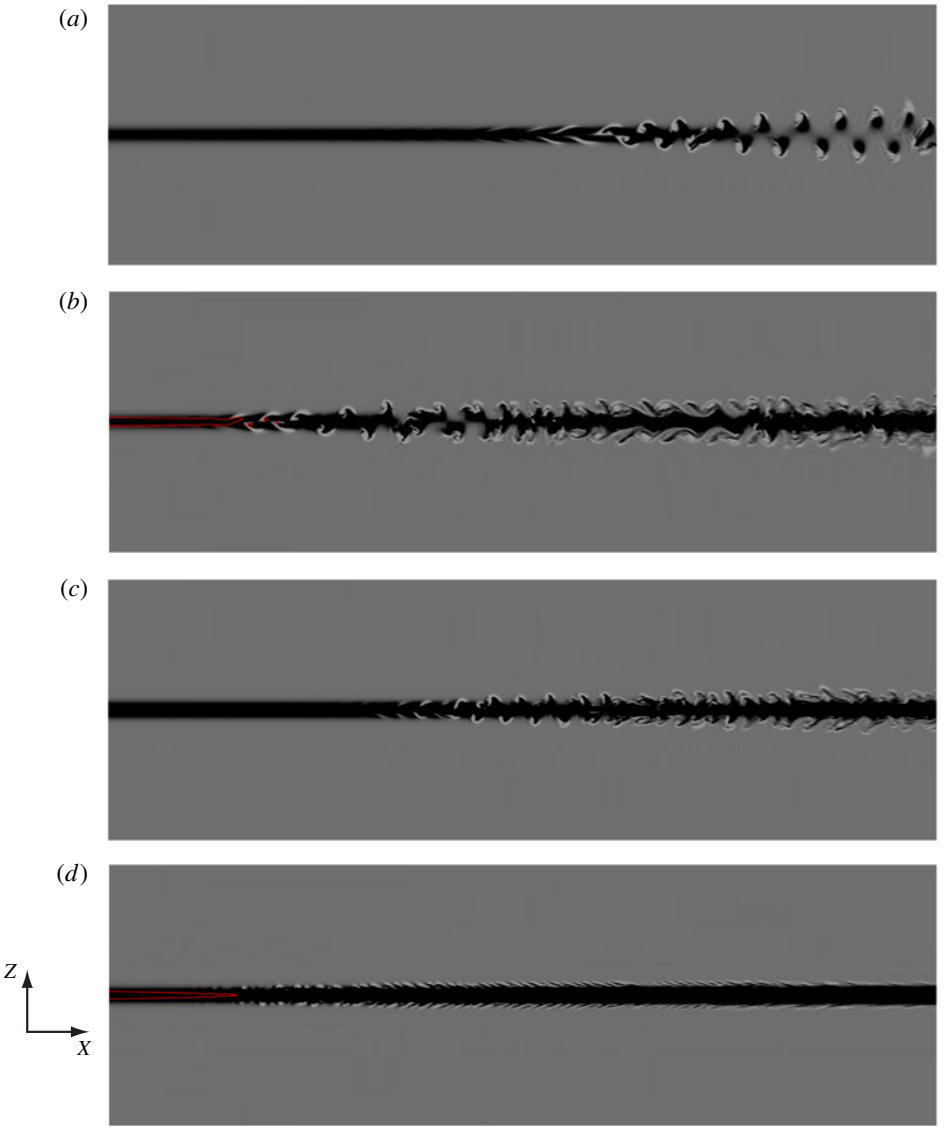


FIGURE 4. Transition processes of the streamwise vortices, described by the helicity density contours in the cross-sections through the vortex axis; (*a*) $\Phi = 0.16$, (*b*) 0.20, (*c*) 0.32 and (*d*) 0.40 at $M_\infty = 3.5$. Positive and negative helicities are rendered in black and white, respectively. Black regions indicate the main vortical structure in the swirling flows; the red lines enclose the subsonic domain.

breakdown occurs, the momentum increase satisfies (3.3) because $\partial u_y/\partial y \approx \partial u_r/\partial r < 0$, which numerically checks that the neglected terms in the right-hand side are small. (Note that u_r is almost zero from upstream to the onset point at the axis.) Another feature of vortex breakdown is the sign change in the azimuthal vorticity ω_θ near the axis (Brown & Lopez 1990). In incompressible flows, this sign change occurs when the axial velocity profile alters from jet-like to wake-like and *vice versa* (Oberleithner *et al.* 2012). For the Batchelor vortex in (2.1), $\omega_\theta = -\partial u_x/\partial r$ at the upstream. If a

https://doi.org/10.1017/jfm.2018.92 Published online by Cambridge University Press

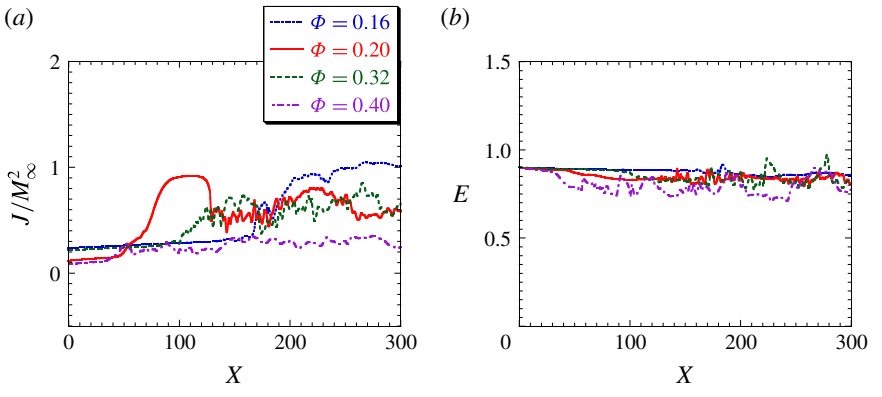


FIGURE 5. Spatial variations of (*a*) axial momentum and (*b*) energy (4.1) along the X-axis in the numerical simulations with $\Phi = 0.16, 0.20, 0.32$ and 0.40 at $M_\infty = 2.5$.

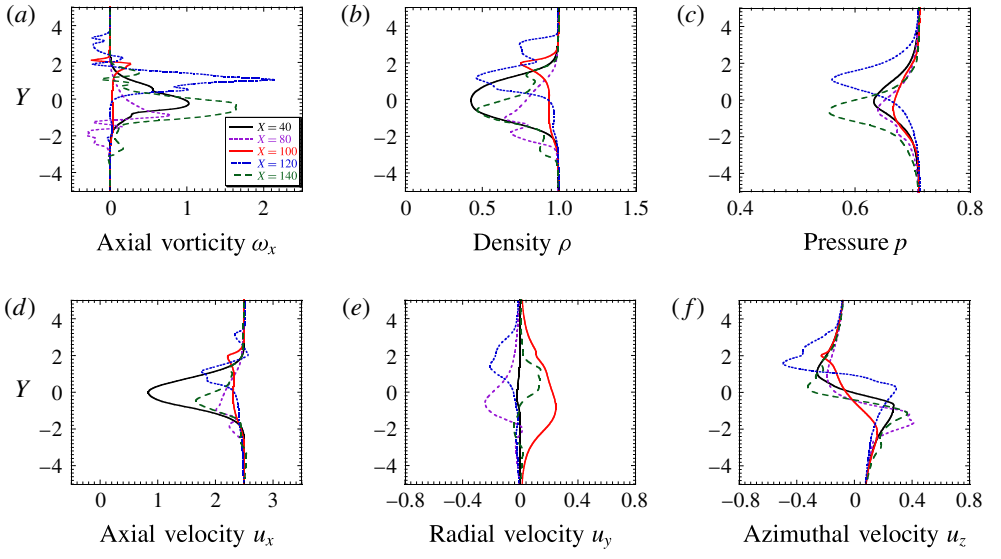


FIGURE 6. Axial vorticity and primitive variables (density ρ, pressure p and velocities u_x, u_y and u_z) in various planes perpendicular to the mainstream flow at $M_\infty = 2.5$ and $\Phi = 0.20$.

positive $\partial u_r/\partial x$ term appears at the downstream, the term produces the opposite sign in the azimuthal vorticity because $\omega_\theta = \partial u_r/\partial x - \partial u_x/\partial r$. In the present case, the u_r component occurs around the breakdown site. As can be seen from the helicity density contours in figure 3(*b*), the opposite sign in ω_θ is described as a white part at the outer region of the vortex core, where ω_x is very small. Thus, the present breakdown also indicates the sign change.

To evaluate the appropriateness of the onset condition in § 3, equation (3.4) was numerically computed for various Φ and M_∞. The results are tabulated in table 1. A positive momentum change indicates the onset of breakdown. Observing this table, it is found that the breakdown condition is fulfilled when Φ is small. As flow fields

https://doi.org/10.1017/jfm.2018.92 Published online by Cambridge University Press

Φ	$M_\infty = 1.5$	$M_\infty = 2.5$	$M_\infty = 3.5$	$M_\infty = 5.0$
0.16	0.1422	0.1831	0.1501	−0.3088
0.20	0.1256	0.1015	−0.07944	−0.5346
0.32	−0.06689	−0.1981	−0.3776	−0.5438
0.40	−0.2744	−0.4818	−0.6152	−0.6645

TABLE 1. Signs of (3.4) under vortex breakdown conditions, obtained from results in the numerical simulations.

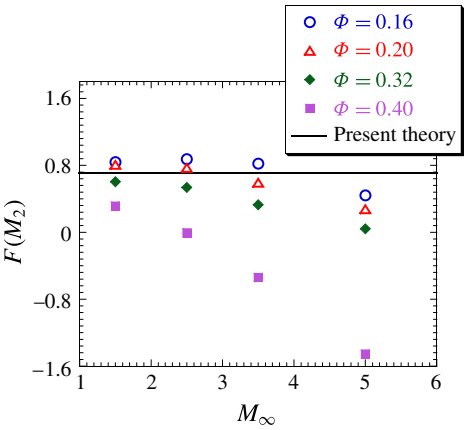


FIGURE 7. Comparison of the theoretical value calculated by (3.11) with the upstream conditions and the values of $F(M_2)$ obtained from numerical simulations for $\Phi =$ 0.16, 0.20, 0.32 and 0.40. When the longitudinal axis exceeds the theoretical threshold value α, vortex breakdown occurs.

in vortex breakdown are subjected to modes with low azimuthal wavenumbers (Ruith *et al.* 2003; Herrada & Fernandez-Feria 2006; Oberleithner *et al.* 2012; Hiejima 2017), the low wavenumber of an unstable mode for small Φ might be an important determiner of breakdown. The five positive results of (3.4) are also consistent with the visualisation results in figures 3 and 4, which reveal regions with no main vortex axis. Therefore, the axial momentum variation calculated by (3.4) can reliably discriminate the presence or absence of vortex breakdown. To enhance further understanding of vortex breakdowns, it might be also necessary to validate the onset condition in vortices other than the Batchelor vortex.

Finally, the threshold M_2 needed for supersonic vortex breakdown was calculated by (3.11). When $F(M_2) > \alpha$, vortex breakdown occurs. The numerical results for various M_∞ and Φ are summarised in figure 7. In the numerical calculations, M_2 was taken as the maximum at the downstream. This stringent condition was chosen because the momentum increases after transition or breakdown. The development of vortex breakdown was suppressed by large swirl parameters Φ and was stabilised by compressibility effects at large M_∞. The same effects were observed in transitions of streamwise vortices (Hiejima 2014). As shown in figure 7, the five positive cases in table 1 satisfy the requirement of M_2 for vortex breakdown, confirming that (3.11) can usefully estimate the threshold M_2 of vortex breakdown without stagnation points. It follows that supposing a downstream pressure in (3.11) is also reasonable.

https://doi.org/10.1017/jfm.2018.92 Published online by Cambridge University Press

5. Concluding remarks

Vortex breakdown comprises a transition between two conjugate states of flow (Benjamin 1962; Mager 1972; Escudier 1988). The axial momentum is not conserved along the axis because the breakdown induces a radial velocity component (Brown & Lopez 1990). A supersonic breakdown configuration appears without a stagnation point, i.e. a spiral-type configuration, accompanied by axial velocity acceleration (Hiejima 2017). From the accumulated knowledge, this study proposes a universal onset condition of vortex breakdowns derived from the axial momentum variation and verifies the condition using three-dimensional numerical simulations of swirling wakes (Batchelor vortices). The theoretical expression is independent of the basic flows and accounts for the increasing momentum in the streamwise direction, which is largely contributed by the breakdown phenomenon. The theoretically predicted and numerically simulated breakdowns were consistent for swirl parameters ranging from 0.16 to 0.40 and Mach numbers ranging from 1.5 to 5.0. Supersonic breakdown occurred when Φ and M_∞ were small, confirming that the derived condition can discriminate the presence or absence of vortex breakdown. Moreover, the expression suggests that bubble breakdown with a stagnation point is unlikely to occur under supersonic conditions ($M_\infty > 1$). The threshold of the downstream Mach number required for supersonic breakdown was also theoretically derived and verified by numerical results. Therefore, the present condition is extensively applicable to the onset of vortex breakdown for a range of speeds.

Acknowledgements

This work was partly achieved through the use of large-scale computer systems SX-ACE at the Cybermedia Centre, Osaka University and was supported by JSPS KAKENHI grant no. JP17K05145. The author expresses his gratitude to the anonymous referees for helping to improve the paper.

References

ABID, M. 2008 Nonlinear mode selection in a model of trailing line vortices. *J. Fluid Mech.* **605**, 19–45.

BATCHELOR, G. K. 1964 Axial flow in trailing line vortices. *J. Fluid Mech.* **20**, 645–658.

BENJAMIN, T. B. 1962 Theory of the vortex breakdown phenomenon. *J. Fluid Mech.* **14** (4), 593–629.

BROADHURST, M. S. & SHERWIN, S. J. 2008 Helical instability and breakdown of a Batchelor trailing vortex. In *Progress in Industrial Mathematics at ECMI 2006, Mathematics in Industry*, pp. 191–195. Springer.

BROWN, G. L. & LOPEZ, J. M. 1990 Axisymmetric vortex breakdown. Part 2. Physical mechanisms. *J. Fluid Mech.* **221**, 553–576.

DARMOFAL, D. L., KHAN, R., GREITZER, E. M. & TAN, C. S. 2001 Vortex core behaviour in confined and unconfined geometries: a quasi-one-dimensional model. *J. Fluid Mech.* **449**, 61–84.

DELERY, J. M. 1994 Aspects of vortex breakdown. *Prog. Aerosp. Sci.* **30**, 1–59.

ESCUDIER, M. 1988 Vortex breakdown: observations and explanations. *Prog. Aerosp. Sci.* **25** (2), 189–229.

HALL, M. G. 1972 Vortex breakdown. *Annu. Rev. Fluid Mech.* **4**, 195–218.

HERRADA, M. A. & FERNANDEZ-FERIA, R. 2006 On the development of three-dimensional vortex breakdown in cylindrical regions. *Phys. Fluids* **18** (8), 084105.

HERRADA, M. A., PÉREZ-SABORID, M. & BARRERO, A. 2003 Vortex breakdown in compressible flows in pipes. *Phys. Fluids* **15** (8), 2208–2218.

HIEJIMA, T. 2013 Linear stability analysis on supersonic streamwise vortices. *Phys. Fluids* **25**, 114103.

https://doi.org/10.1017/jfm.2018.92 Published online by Cambridge University Press

HIEJIMA, T. 2014 Spatial evolution of supersonic streamwise vortices. *Phys. Fluids* **26**, 074102.

HIEJIMA, T. 2016 Effects of streamwise vortex breakdown on supersonic combustion. *Phys. Rev.* E **93**, 043115.

HIEJIMA, T. 2017 Streamwise vortex breakdown in supersonic flows. *Phys. Fluids* **29**, 054102.

KELLER, J. J. 1994 On the practical application of vortex breakdown theory to axially symmetrical and three-dimensional compressible flows. *Phys. Fluids* **6** (4), 1515–1523.

LEIBOVICH, S. 1978 The structure of vortex breakdown. *Annu. Rev. Fluid Mech.* **10**, 221–246.

LUCCA-NEGRO, O. & O'DOHERTY, T. 2001 Vortex breakdown: a review. *Prog. Energy Combust. Sci.* **27**, 431–481.

LUGINSLAND, T. & KLEISER, L. 2015 Mach number influence on vortex breakdown in compressible, subsonic swirling nozzle-jet flows. In *Direct and Large-Eddy Simulation IX*, pp. 311–317. Springer.

MAGER, A. 1972 Dissipation and breakdown of a wing-tip vortex. *J. Fluid Mech.* **55** (4), 609–628.

MAHESH, K. 1996 A model for the onset of breakdown in an axisymmetric compressible vortex. *Phys. Fluids* **8** (12), 3338–3345.

NELSON, R. C. & PELLETIER, A. 2003 The unsteady aerodynamics of slender wings and aircraft undergoing large amplitude maneuvers. *Prog. Aerosp. Sci.* **39** (2), 185–248.

OBERLEITHNER, K., PASCHEREIT, C. O., SEELE, R. & WYGNANSKI, I. 2012 Formation of turbulent vortex breakdown: intermittency, criticality, and global instability. *AIAA J.* **50** (7), 1437–1452.

RUITH, M. R., CHEN, P., MEIBURG, E. & MAXWORTHY, T. 2003 Three-dimensional vortex breakdown in swirling jets and wakes: direct numerical simulation. *J. Fluid Mech.* **486**, 331–378.

RUSAK, Z. & LEE, J. H. 2002 The effect of compressibility on the critical swirl of vortex flows in a pipe. *J. Fluid Mech.* **461**, 301–319.

SHTERN, V. & HUSSAIN, F. 1999 Collapse, symmetry breaking, and hysteresis in swirling flows. *Annu. Rev. Fluid Mech.* **31** (1), 537–566.

VISBAL, M. R. & GORDNIER, R. E. 1995 Compressibility effects on vortex breakdown onset above a 75° sweep delta wing. *J. Aircraft* **32**, 936–942.

https://doi.org/10.1017/jfm.2018.92 Published online by Cambridge University Press